

# Wind Tunnel Investigation of Crow Instability

B. G. Eliason,\* I. S. Gartshore,† and G. V. Parkinson‡  
*University of British Columbia, Vancouver, B. C., Canada*

The mutual instability of a trailing vortex pair has been studied in a large wind tunnel. The vortices were visualized using helium-filled soap bubbles and the cores probed with a hot-wire anemometer. Measurements were made to permit calculation of the wing lift, the circulation of the trailing vortices, the diameter of the vortex cores, and the wavelength and plane of oscillation of the unstable vortices. The results show that the linear theories of either Crow or Parks closely predict the characteristics of the instability, the agreement depending on the definition of the vortex core diameter.

## Nomenclature

$a$	= rate of displacement amplification
$\mathcal{R}$	= wing aspect ratio
$b$	= original vortex separation
$c$	= vortex core diameter
$C_D$	= wing drag coefficient
$C_L$	= wing lift coefficient
$E$	= linearized anemometer output
$r$	= radial distance from vortex center
$s$	= wingspan
$t$	= time
$T$	= time for wave amplitude to grow by factor $e$
$V_0$	= aircraft speed
$\alpha_a$	= angle of attack
$\alpha_s$	= nondimensional amplification rate of symmetric mode ( $2\pi b^2/\Gamma$ ) $a$
$\beta$	= nondimensional wave number $2\pi b/\lambda$
$\Gamma$	= circulation around vortex
$\Gamma_0$	= circulation at midspan of wing
$\lambda$	= wavelength of disturbance
$\rho$	= density of air

## Introduction

THE problem of wake turbulence, the persistence of the pair of trailing vortices behind large aircraft, has been receiving wide attention in the last few years because of the considerable number of aircraft accidents it is believed to have caused. There is a continuing need for better understanding of the process of formation and dissipation of these trailing vortices. One of the several processes for the breakup of a trailing vortex pair arises from a mutual instability of the pair. This instability process, in which the vortices develop a sinusoidal waveform whose amplitude grows until the two vortices link and form vortex rings, has been observed qualitatively on numerous occasions in actual aircraft flight,<sup>1</sup> and is the subject here. Detailed quantitative measurements possible in the controlled environment of a long wind tunnel are reported, essentially to substantiate the hypotheses made in analytical models of the process.

The fundamental theoretical model of the instability process was developed by Crow.<sup>2</sup> He presented a linear stability theory in which the vortices are idealized as potential line vortices, and the effects of the actual finite core diameter are accounted for by a cutoff in the integral representing the self-induced velocity of a filament. Subsequent refinements by others<sup>3,4</sup> have accounted directly for the effects of finite core size, vorticity distribution, and axial velocities.

However, experimental verification of the theory has been slow in appearing. Flight tests such as those described in Ref. 1, have provided good qualitative verification of some of the predicted phenomena, but such tests are expensive and difficult to make quantitative, largely because of unpredictable atmospheric effects. Conventional wind tunnels with short test sections do not lend themselves to model studies of a trailing vortex system. There have been a few flow visualization model studies, one using a piston-generated vortex pair in a special water tank,<sup>4</sup> several using a water-filled towing tank,<sup>5-7</sup> and others towing a lifting wing through the air.<sup>8,9</sup>

The present investigation made use of the 80-ft long test section of the new University of British Columbia low-speed wind tunnel. The trailing vortices of a lifting wing mounted at the upstream end were visualized and measurements made to permit calculation of the wing lift, the circulation of the trailing vortices, the diameter of the vortex cores, and the wavelength and plane of oscillation of the disturbed vortices. Effects of artificial excitation of the instability were also studied.

## Review of Stability Theory Results

In Crow's linear stability theory,<sup>2</sup> the amplification of the vortices is exponential, and depends primarily on the dimensionless wave number  $\beta = 2\pi b/\lambda$  where  $b$  is the vortex separation and  $\lambda$  is the wavelength of the disturbance. He used an additional variable, the effective size of the rotational vortex cores, to determine the truncation of certain self-induction integrals, so that his results agreed favorably with known solutions to similar problems.

Parks<sup>3</sup> accounted for the finite core diameter more directly by generalizing Crow's analysis to include a core of uniform vorticity. In both cases, the results are expressed as  $\alpha_s$ , the nondimensional amplification rate, as a function of  $\beta$ , with the effective core diameter  $c$  (nondimensionalized by the vortex separation  $b$ ) as a parameter. Physically,  $\alpha_s$  is the actual amplification rate  $a$  where growth is given by  $\exp(at)$ , multiplied by the time taken by the vortices to drift downward a distance equal to  $b$ , their initial separation. Ground effects are not considered.

## Experimental Method

According to Crow's theory, the wave amplitude increases by a factor  $e$  in a time  $T$  proportional to  $b^2/\Gamma$ , or, in terms of aircraft parameters, proportional to  $(\mathcal{R}/C_L)b/V_0$  where  $b$  is the vortex separation, somewhat less than the span  $s$ ,  $\Gamma$  is the circulation of each vortex,  $\mathcal{R}$  is the wing aspect ratio,  $C_L$  is the wing lift coefficient, and  $V_0$  is the aircraft speed. To hasten the growth of the instability in the present experiment,  $C_L$  was chosen as large as possible,  $s$  was chosen to be small, and  $\mathcal{R}$  was chosen to be small but still not unrealistic. The airfoil section chosen was the NACA 23021 with 40% chord

Received August 26, 1974; revision received March 11, 1975.

Index categories: Aircraft Aerodynamics (including Component Aerodynamics); Nonsteady Aerodynamics.

\*Graduate Student, Department of Mechanical Engineering.

†Associate Professor, Department of Mechanical Engineering.

‡Professor, Department of Mechanical Engineering.

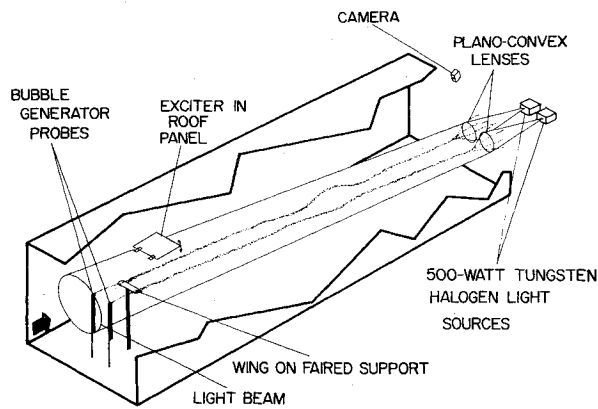


Fig. 1 Experimental setup.

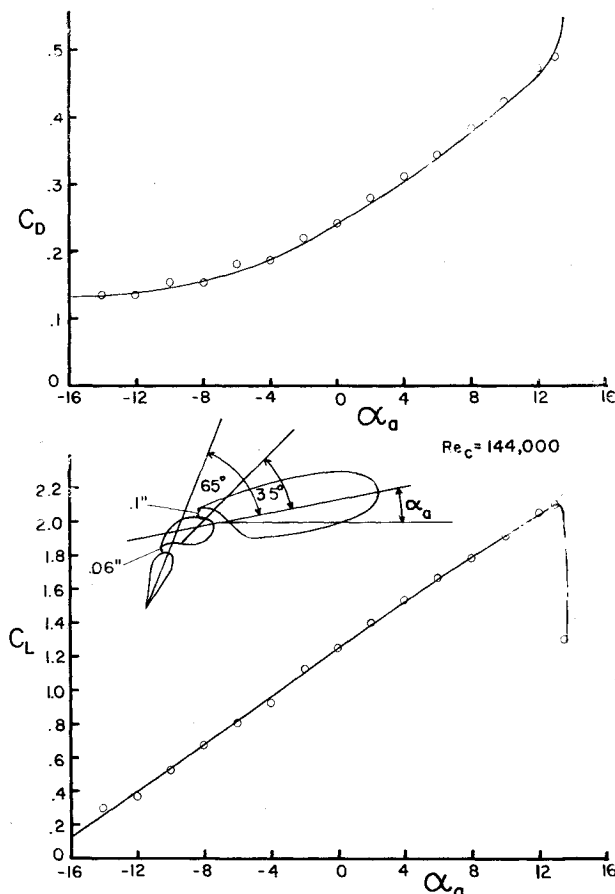


Fig. 2 Lift and drag curves for model with flap spacing and deflections to produce maximum lift.

double slotted flaps. This gives a sectional lift coefficient in excess of 3.4 at high Reynolds number.<sup>10</sup> The span and chord were chosen to be 12 and 3 in., respectively, giving an aspect ratio of 4. The model endplates and template were machined on a numerically controlled milling machine and the model was built of mahogany. The tunnel test section dimensions are 5 ft-3 in.  $\times$  8 ft  $\times$  80 ft, so wall corrections were considered unnecessary. The tunnel turbulence level is 0.35%.

The wing was tested in a smaller wind tunnel, where lift and drag were measured for various flap angles and spacings. From these results, the optimum settings were chosen and used throughout the remainder of the tests. The model was mounted from a single faired support at midspan.

Helium-filled soap bubbles were used to make the vortices visible. The commercially available bubble generator<sup>11</sup> produced approximately 500 bubbles per sec varying in size from 1/32 to 1/8 in. The buoyancy of the bubbles in air

ranged from slightly negative to slightly positive. Although the heavier bubbles tended to be thrown out of the vortex flow, the lighter ones gravitated to the centers of the vortices, rendering the cores visible for long distances. The bubbles were extremely durable, withstanding high levels of turbulence. The bubble trails, although visible to the naked eye, proved impossible to photograph without special lighting. A pair of 500-w tungsten-halogen light sources, each with a large plano-convex lens, was used to provide high-intensity light beams which could be shone down the test section. A diagram of the experimental setup is shown in Fig. 1.

A hot-wire anemometer was used to traverse the vortex to determine the vortex core diameters at two downstream positions. The core diameters are used as an input to the stability theories. Artificial disturbances also could be created using an oscillating panel mounted in the roof just downstream of the model. The trailing vortices experienced the potential flowfield of this oscillating panel, but were not in its wake. The tests were run at wind speeds of 60 and 70 fps, giving chord Reynolds numbers of  $1.24 \times 10^5$  and  $1.44 \times 10^5$ .

## Results

The lift and drag curves for the model with optimum flap spacing are shown in Fig. 2. The curves have been corrected to eliminate the effect of the model support.  $C_{Lmax}$  is lower than that predicted by the section characteristics because of the finite  $R$  and the order of magnitude difference in Reynolds number. The lift curve slope, 0.069/deg compares favorably with that predicted theoretically for a rectangular wing of  $R = 4$ , 0.070/deg.<sup>12</sup> The sudden stall characteristic made it necessary to operate at an angle of attack  $2^\circ$  less than that at stall, i.e.,  $C_L = 1.95$ .

The theoretical value of  $b$  for a rectangular wing of  $R = 4$  has been calculated<sup>12</sup> as 0.854s. The corresponding circulation  $\Gamma_0$  at midspan of the wing calculated from the measured lift is 17.1 ft<sup>2</sup>/sec. The actual circulation  $\Gamma$  of the trailing vortices was measured by their rate of downward mutual induction. The vortices had dropped 27 in. in a distance of 75 ft at a tunnel speed of 60 fps.  $\Gamma$  as calculated by this method was 9.7 ft<sup>2</sup>/sec or 57% of  $\Gamma_0$ . This measurement is in agreement with those of other investigators.<sup>13-15</sup> Once the trailing vortices were a few chords behind the wing, beyond the effect of the bound vorticity of the wing, the sink rate became constant. This observation implies that the total amount of vorticity did not change appreciably within the length of the test section, even though the distribution of this vorticity may have changed. At the test section exit, the distance of the vortices to the tunnel floor was approximately  $1.8b$ . At this point, the ground-effect-induced velocity is less than 10% of the mutual induction velocity, so it is felt that ground effects can be neglected.

The measurement of the vortex core diameter  $c$  was accomplished by aligning the hot-wire axis with the mean flow.

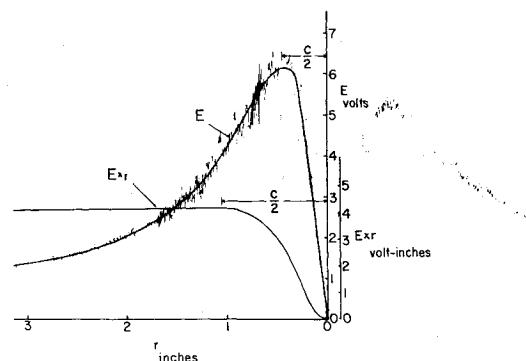


Fig. 3 Typical anemometer traverse of vortex 32 chords downstream of wing showing two methods of defining core diameter. Traverse is perpendicular to span and begins from left.

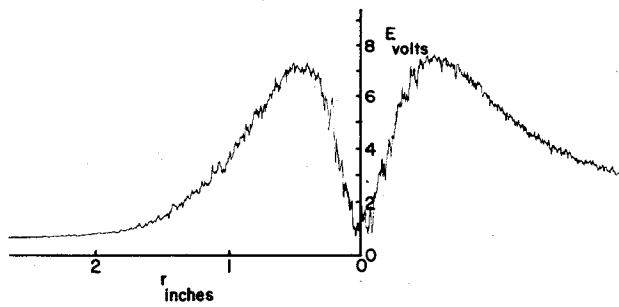


Fig. 4 Typical anemometer traverse of vortex 4 chords downstream. Scale of ordinate is different but the direction of traverse is same as that in Fig. 3.

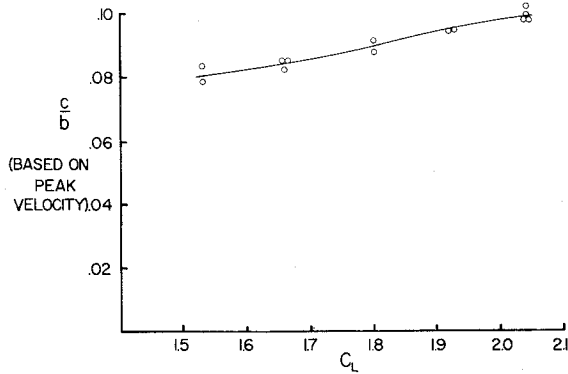


Fig. 5 Effect on core diameter of varying  $C_L$ .

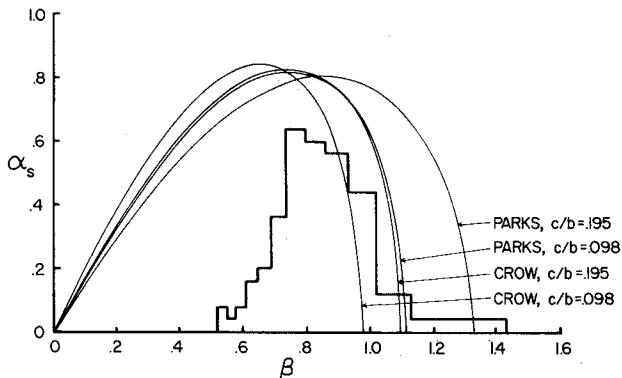


Fig. 6 Theoretical nondimensional amplification rates for two theories using two core diameter definitions. Histogram shows relative frequency of occurrence of 84 experimentally measured symmetric waveforms.

As the probe was traversed through the vortex, the effect of the tangential velocity component could be clearly seen on the anemometer output. Figure 3 shows a typical traverse 32 chords downstream of the wing. Although this method cannot be relied upon to give any quantitative information on tangential velocity because of the possibility of varying axial velocities in the vortex, it does define the core region very accurately. The effect of probe contamination on the signal, although weak, was increasingly noticeable as the probe passed through the center of the core. To ensure this was not due to vortex asymmetry the flow was probed from the opposite side. The results showed the vortex to be symmetrical. Also included in Fig. 3 is the product of the linearized anemometer output  $E$  and the radial distance  $r$ . This product which is related to the circulation contained within a given radius, can be used in defining the core diameter.

One can define the core diameter in a number of ways. One would be to let  $c$  be the approximate mean diameter of the transition zone from the core solid-body rotation to the outer irrotational field, as measured from the peaks of the velocity

Fig. 7 Photo from above looking upstream showing filament instability.

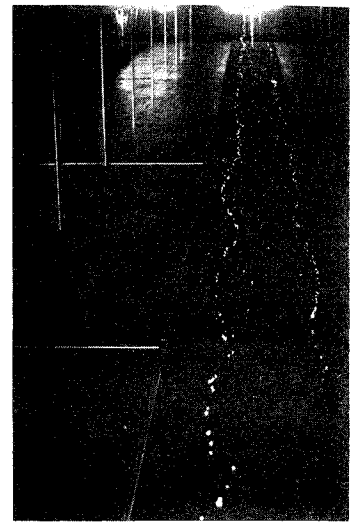


Fig. 8 Photo from above looking upstream with exciter in operation. The image shows a dark, elongated vortex core with a bright, irregular filament trailing behind it, similar to Fig. 7 but with more pronounced oscillations.

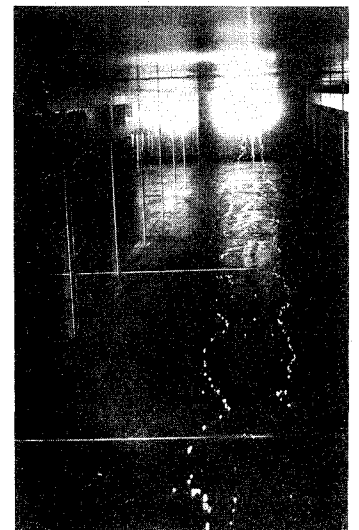
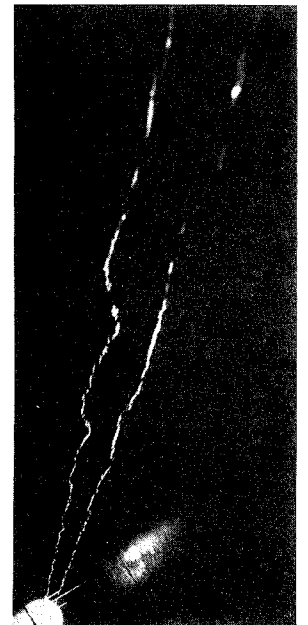


Fig. 9 Photo taken at  $45^\circ$  to the horizontal; One bubble trail appears as a straight line, indicating that plane of oscillation is close to  $45^\circ$ .



curve. This method, however, neglects the vorticity distributed outside of this region. A second approach would define the core diameter to be that region in which all of the measurable vorticity lay, as determined by the points at which

$E \cdot r$  becomes constant. Both definitions are used and their effects on theoretical predictions are compared.

The core diameters were measured at two downstream positions, 4 chords and 32 chords as measured from mid-chord. A typical traverse at 4 chords is shown in Fig. 4. At this position the anemometer output did not vary inversely with radius. This may be due to strong axial velocity gradients or incomplete rollup. At the 32-chord position,  $E$  does vary as  $1/r$ , (Fig. 3), implying a flowfield much closer to the potential vortex model. The flow could not be probed at greater downstream distances, due to unsteadiness of the vortex position.

The core diameter based on peak velocity was 1.0 in. or  $0.098b$ . This value is only half that predicted by Spreiter and Sachs,<sup>16</sup> ( $0.197b$ ), but is greater than the values found by other investigators using wings with much lower lift coefficients.<sup>14,17</sup> The effect of varying  $C_L$  on core diameter is shown in Fig. 5. These results, from data similar to Fig. 4, were taken at the 4-chord position and because they could only be measured from peak to peak and are affected by probe contamination, they should be accepted only as a qualitative indication of the effect of varying  $C_L$ . From the 4-chord position to the 32-chord position, the core diameter had grown by 2.4%. Defining  $c$  as the diameter which includes 100% of the measurable vorticity (Fig. 3) gives  $c = 2.1$  in. or  $0.195b$ . The measured core diameter thus varies from  $0.098b$  to  $0.195b$ , depending on the definition of the core.

Using the two measured values of  $c/b$ , Crow's expression for  $\alpha_s$  as a function of  $\beta$  is shown in Fig. 6. Parks' expression for  $\alpha_s$  for the same two values of core diameter has also been plotted in Fig. 6. In each case, the wave which will grow most quickly has the wave number  $\beta$  corresponding to the point at which the curve peaks.

The vortices, made visible by the bubbles, were photographed from above, using 35-mm still and high-speed 16-mm motion pictures (Fig. 7). Measurements of the wavelengths were made by photographing a graduated string placed in the same position as that in which the vortices were photographed. Only 10% of these photos showed measurable disturbances and only those waves which were clearly sinusoidal symmetric waves were measured. The wave numbers of 84 such waves are shown in the histogram in Fig. 6.

Varying the lift coefficient during the tests produced no noticeable effect on the measured wavelengths. There were generally fewer waves produced at the lower value of  $C_L$ . Exciting the vortices in the neighborhood of  $\beta = 0.85$  produced waves of much larger amplitude, as shown in Fig. 8. The larger amplitudes are a result of energy being added to the wake at a wave number corresponding to the maximum wave growth rate, thus exciting the most unstable form of wave more quickly. The plane of oscillation was measured with the exciter in operation to take advantage of the larger amplitude and more periodic nature of the waves. Figure 9 shows a photo taken at an angle of  $45^\circ$  to the horizontal. This and similar photos confirmed that the plane of oscillation lay between  $40^\circ$  and  $50^\circ$  to the horizontal. The result is in good agreement with the  $48^\circ$  prediction of the linear theory.

### Discussion

In comparing the theoretical and experimental results in Fig. 6, it should be kept in mind that theoretical ordinates are amplification rates, whereas the experimental histogram merely gives the observed frequency of occurrence of various wave numbers. The confirmation of the theory lies in the fact that it predicts the waves with maximum amplification rates to be the most probable. Comparing the two stability theories shows that the Parks refinement to the Crow model gives a slightly better fit to the experimental data using the peak-to-peak definition of core diameter, but Fig. 6 also indicates that each theory can predict the results equally well by choosing an appropriate core diameter. The wavelengths measured show excellent agreement with the full-scale measurements of Chevalier.<sup>1</sup>

The half-amplitudes of the largest waves produced without artificial excitation were of the order of  $0.2b$  at the end of the test section, about 40 times larger than could be explained by assuming direct response of the vortices to the low-intensity turbulent fluctuations of the tunnel flow. Considerably larger amplitudes were produced when the roof panel exciter was oscillated at a frequency to correspond with  $\beta$  near 0.85. This observation shows the importance of disturbance frequencies near the critical value of  $\beta$  and suggests that the presence of disturbances in this frequency range, either in atmospheric turbulence or introduced artificially from the aircraft, would reduce the time required for the vortices to link.

During the entire test program, the vortex bursting phenomena observed by others<sup>5,18</sup> were never observed. In addition, the instabilities were all of the long wavelength type and none of the short waves noted in Ref. 4 were observed.

### Conclusions

The above experimental results show that the mutual instability of a trailing vortex pair can be observed in the wind tunnel, and the measured wavelengths and plane of oscillation show that the linear stability theory provides a good description of the initial growth of the waves. Both the Crow theory and the Parks modification to it give equally good agreement with the experimental data, depending on the definition of core diameter used in each case.

### References

- 1 Chevalier, H., "Flight Test Studies of the Formation and Dissipation of Trailing Vortices," *Journal of Aircraft*, Vol. 10, Jan. 1973, pp. 14-18.
- 2 Crow, S. C., "Stability Theory for a Pair of Trailing Vortices," *AIAA Journal*, Vol. 8, Dec. 1970, pp. 2172-2179.
- 3 Parks, P. C., "A New Look at the Dynamics of Vortices with Finite Cores," *Aircraft Wake Turbulence and Its Detection*, Olsen, J. H. et al. (ed.), Plenum Press, New York, 1971, pp. 355-388.
- 4 Widnall, S. E., Bliss, D., Zalay, A., "Theoretical and Experimental Study of the Stability of a Vortex Pair," *Aircraft Wake Turbulence and Its Detection*, Olsen, J. H., et al., (ed.), Plenum Press, New York, 1971, pp. 305-338.
- 5 Olsen, J. H., "Results of Trailing Vortex Studies in a Towing Tank," *Aircraft Wake Turbulence and Its Detection*, Olsen, J. H., et al., (ed.), Plenum Press, New York, 1971, pp. 455-472.
- 6 Hackett, J. E. and Theisen, J. G., "Vortex Wake Development and Aircraft Dynamics," *Aircraft Wake Turbulence and Its Detection*, Olsen, J. H., et al., (ed.), Plenum Press, New York, 1971, pp. 243-263.
- 7 Withycombe, E., "Wingtip Vortex Decay: An Experimental Investigation," S.B. Thesis, M.I.T., 1970 (as referenced in Ref. 4).
- 8 Kiang, R. L., "Subscale Modeling of Aircraft Trailing Vortices," *Aircraft Wake Turbulence and Its Detection*, Olsen, J. H., et al., (ed.), Plenum Press, New York, 1971, pp. 81-95.
- 9 Patterson, J. C., Jr., "Lift-Induced Wing-Tip Vortex Attenuation," *Journal of Aircraft*, Vol. 12, Sept. 1975, pp. 745-749.
- 10 Harris, T. A. and Recant, I. G., "Wind-Tunnel Investigation of NACA 23012, 23021, and 23030 Airfoils Equipped with 40% Chord Double Slotted Flaps," NACA Rep. 723, 1941, pp. 321-347.
- 11 Ordway, D. E., Sage Action Inc., Ithaca, N.Y.
- 12 Glauert, H., *Elements of Aerofoil and Aircrew Theory*, Cambridge University Press, New York, 1930, Chaps. 11, 12.
- 13 Mason, W. H. and Marchman, J. R. III, "Far-field Structure of Aircraft Wake Turbulence," *Journal of Aircraft*, Vol. 10, Feb. 1973, pp. 86-92.
- 14 Grow, T. L., "Effect of a Wing on Its Tip Vortex," *Journal of Aircraft*, Vol. 6, Jan.-Feb. 1969, pp. 37-41.
- 15 Dosanjh, D. S., Gasperek, E. P., Eskinazi, S., "Decay of a Viscous Trailing Vortex," *Aeronautical Quarterly*, May 1962, pp. 167-188.
- 16 Spreiter, J. R. and Sachs, A. H., "The Rolling Up of the Trailing Vortex Sheet and Its Effect on the Downwash Behind Wings," *Journal of the Aeronautical Sciences*, Vol. 18, Jan. 1951, pp. 21-32.
- 17 Rorke, J. B. and Moffitt, R. C., "Wind-Tunnel Simulation of Full-Scale Vortices," NASA Contractor Rept. NASA CR-2180, 1973.
- 18 Tombach, I., "Observations of Atmospheric Effects on Vortex Wake Behavior," *Journal of Aircraft*, Vol. 10, Nov. 1973, pp. 641-647.